NACA

RESEARCH MEMORANDUM

OBSERVATIONS ON AN AILERON-FLUTTER INSTABILITY ENCOUNTERED

ON A 45° SWEPT-BACK WING IN TRANSONIC AND SUPERSONIC FLIGHT

By

Marvin Pitkin, William N. Gardner
and Howard J. Curfman, Jr.

Langley Memorial Aeronautical Laboratory
Langley Field, Va.

CLASSIFICATION CANCELLED

Authority naca RN 2344 Date 8/18/54

n.t.n 8/31/54 See

NATIONAL ADVISORY COMMITTEE
FOR AERONAUTICS
WASHINGTON
April 11, 1947

UNCLASSIFIED

CONFIDENTIAL

3 1176 01437 0200

NACA RM No. L6L09

NATIONAL ADVISORY COMMITTEE FOR AERONAUTICS

RESEARCH MEMORANDUM

OBSERVATIONS ON AN AILERON-FLUTTER INSTABILITY ENCOUNTERED ON A

45° SWEPT-BACK WING IN TRANSONIC AND SUPERSONIC FLIGHT

By Marvin Pitkin, William N. Gardner
and Howard J. Curfman, Jr.

SUMMARY

In the course of a flight test of a supersonic research
pilotless aircraft (the NACA RM-1), large-amplitude aileron
oscillations, probably aileron compressibility flutter, were
encountered in the transonic and supersonic speed ranges. The
wing was oscillating at the same frequency as the aileron. The
aircraft was equipped with 45° swept-back wings of symmetrical
NACA 65-010 airfoil section. Completely mass-balanced ailerons
with 20° beveled trailing edges were installed on the wings. The
ailerons were free floating with no mechanical restraining force
other than the friction of the aileron hinges and servomechanism
bearings throughout the high-speed interval of flight.

Flight data are presented showing the free-floating and
oscillatory characteristics of the wing and aileron throughout
the flight. It is shown that aileron vibration occurred at flight
velocities corresponding to a Mach number range from 1.03 to 1.4.
The frequencies of the aileron and wing oscillations were identical
at a given Mach number, were of the order of 100 cycles per second,
and increased with Mach number. The test data indicate that aileron
compressibility flutter, considered as a phenomenon associated with
the flow pattern at supercritical Mach numbers, is delayed in
appearance but not prevented by sweepback. At high subsonic speeds
the data indicated that the beveled-edge aileron was underbalanced
at large deflections and overbalanced at small deflections. At
Mach numbers above 0.90, however, the aileron became overbalanced
over a larger deflection range until a Mach number of 0.95 was
reached. Above a Mach number of 0.95 the aileron became definitely
underbalanced.

INTRODUCTION

A standard RM-1 stability and control research pilotless aircraft, completely described in reference 1, was equipped with a wing rolling-moment balance and a control-position indicator for the purpose of measuring the rolling moments produced by aileron deflection at transonic and supersonic speeds. During the flight of this model, the internal power supply to the automatic pilot and aileron servomechanisms failed. After the power failure, the automatic pilot and aileron servomechanisms became inoperative, and the ailerons were left free floating with no mechanical restraining force other than the friction of the aileron hinges and servomechanism bearings.

The telemeter data obtained from this flight indicate that the wings and ailerons experienced high-frequency oscillations in the transonic and low supersonic speed ranges. Although this flight was not intended to be a flutter or vibration investigation, the results of the test are presented at this time in view of the current interest in aileron compressibility flutter experienced on high-speed airplanes.

SYMBOLS

L rolling moment; positive to the right

δ_a aileron deflection; positive when causing roll to the right

g acceleration of gravity, 32.2 feet per second per second

M Mach number

APPARATUS AND MODEL

Model

The standard RM-1 stability and control research model consists of a cylindrical body of fineness ratio 22.7 equipped with four cruciform wings and four cruciform fins. The wings and fins are swept back 45° and are of constant chord NACA 65-010 airfoil section normal to the leading edge. Figure 1 is a photograph of the RM-1 model, equipped with a booster rocket, mounted on its launching rack. The model, booster, and launching equipment are completely described in reference 1.

Two diametrically opposite wings are equipped with ailerons.
Figure 2 is a photograph of the wing-aileron combination, and
figure 3 is a sketch showing the detail dimensions of the wing
and aileron. The ailerons are 0.10 wing chord, 0.33 wing semispan,
and 100-percent mass balanced; they have a 20° beveled trailing edge
and a moment of inertia of 0.0000102 slug-feet squared about the
hinge line. Stops are provided on the ailerons to limit their
travel to $\pm 10^\circ$.

Electromagnetic servomechanisms are used to actuate the ailerons
which function as a flicker-type control; that is, they are
deflected in either one extreme position or the other at all times.
The sense of deflection is determined by a roll-stabilization
automatic pilot described in reference 1.

Instrumentation

A four-channel telemeter was installed in the model to transmit
intelligence on longitudinal acceleration, impact pressure, angle of
bank, rolling moment, and aileron position. Longitudinal
acceleration and impact pressure were alternately transmitted on
one channel by means of a switching motor. Continuous-wave
Doppler radar apparatus was used to obtain velocity data.
This apparatus transmits a continuous-wave radar signal which is
merged with or "beat against" its reflected echo from a moving
object to yield a record from which the velocity of the moving
body is determined. Reference 1 describes the telemeter equipment
and continuous-wave (C.W.) Doppler radar equipment and presents
methods for obtaining velocity from longitudinal acceleration,
impact pressure, and radar data.

Special Equipment

A control-position indicator was installed on the aileron
servomechanism. Figure 4 is a sketch of the aileron, servomechanism,
and position-indicator arrangement. Although the indicator was not
mounted directly on the aileron because of space limitations, the
instrument was calibrated in terms of aileron deflection. Only
one of the two ailerons was equipped with a position indicator.

The two wings with ailerons were rigidly mounted on the free
end of a steel cantilever spring which served as the rolling-moment
balance. Figure 5 is a schematic sketch of the balance system.
Deflections of the spring are measured by means of a telemeter pickup
and are calibrated in terms of rolling moment. No provision was
made for damping the oscillations of this balance system.

RESULTS AND DISCUSSION

When the sustaining rocket was fired, the power supply to the aileron servomechanisms, automatic pilot, and telemeter switching motor failed. Thereafter, the ailerons were free floating and the automatic pilot became inoperative, thus invalidating the angle-of-bank data. After the power failure, the switching motor stopped, allowing transmission of acceleration data only. These data in addition to rolling-moment and control-position data were consequently the only items measured for most of the duration of the flight.

Figure 6 is a plot of longitudinal acceleration against time for the initial and high-speed interval of the flight. These data were converted to the velocity values shown in figure 7 by the method of reference 1. Also plotted on figure 7 are corresponding velocity data obtained from C. W. Doppler radar and from total-pressure measurements obtained prior to power failure. The velocity data show that the RM-1 model reached a peak velocity of 1570 feet per second which corresponded to a Mach number of 1.395. Agreement between velocity values obtained by the various techniques was good.

Power-On Flight

Telemeter records showed that normal operation of the ailerons and automatic pilot was experienced prior to the power failure. The model stabilized in roll during this period, and a rolling oscillation of $\pm 3.5^\circ$ amplitude was obtained up to the time the sustaining rocket ignited (5.8 seconds). After this time, the control was free floating. Figure 8(a) shows the aileron behavior and Mach number variation for the time the sustaining rocket was firing. These data are cross-plotted in figure 8(b) to show the variation of control deflection with Mach number.

The data presented in figure 8(b) show that when power failed (M = 0.6 approx.) the control was at full deflection and was slightly underbalanced in this deflection range as shown by its drift back toward neutral position. At higher subsonic velocities (M = 0.8 to 0.9) the control trimmed at a constant deflection of approximately -2.3° indicating thereby that the control was over-balanced at smaller deflections. The possibility that the -2.3° deflection is the result of out-of-trim moments has been considered; however information to be presented later herein discounts this possibility. The tendency of the control to over-balance at small deflections is characteristic of beveled-edged controls

and is associated with boundary-layer effects upon the pressures over the trailing-edge bevel. Reference 2 presents a comprehensive discussion of this phenomenon.

At Mach numbers between 0.90 and 0.95 the floating angle of the aileron increased abruptly indicating overbalance over a larger deflection range. A further increase in velocity reversed this effect and the control quickly returned to its neutral position remaining there until the peak Mach number of 1.395 was reached.

The tests reported in reference 1 show that the RM-1 aircraft experiences marked drag rises associated with shock formation at a Mach number of approximately 0.95. The overbalancing of the control at Mach numbers slightly less than this value is thought to be associated with the thickening-boundary-layer effects and flow-separation effects as shock forms on the wing. Reference 3 (p. 62) shows that increasing boundary-layer thickness increases the balance of trailing-edge controls - largest increases in balance being evidenced by controls with large trailing-edge angles. Tests of a P-63A-6 airplane (reference 4) show a large increase in balance of an aileron control at slightly subcritical speeds, similar to that observed in the subject test. Reference 4 ascribes the phenomena to flow separation accompanying assymetrical shock formation upon the upper and lower wing surfaces.

The stiffening of the RM-1 aileron control at supercritical and supersonic speed is probably due to the usual redistribution of chordwise loads in a rearward direction induced by the establishment of supersonic flow conditions over the wing.

Coasting Flight

After the sustaining rocket ceased firing and precisely at the time the forward acceleration passed through zero, a violent high-frequency oscillation occurred on the aileron and wing. The failure of the ailerons to vibrate during the accelerated portion of the flight probably can be attributed to the restraining forces in the servomechanisms which were mounted in such a manner that the large forward accelerations of 6g to 8g could increase their friction considerably. Once the oscillation occurred, however, the friction forces caused by the small decelerations in coasting flight apparently had little influence upon the aileron behavior.

Figure 9(a) shows a time history of the aileron behavior in coasting flight, and in figure 9(b) these data are rearranged to show the variation of aileron deflection with Mach number.

The data presented in figure 9(b) show that the aileron
oscillated with an amplitude of full ±10° deflection over the
entire supersonic range of velocities. As the velocity fell below
a value corresponding to a Mach number of 1.03, erratic aileron
behavior was observed in the transonic region, and at subsonic
speeds the aileron again floated at a small deflection of 2.4°.
This deflection is approximately equal to the trim deflection noted
at subsonic speeds in accelerated flight; however the deflection is
now positive rather than negative and therefore substantiates the
idea that the deflection indicates overbalance of the control and
not merely an out-of-trim position.

A high-frequency wing oscillation accompanied the aileron
oscillation at all times. The characteristics of this wing
oscillation as evidenced by rolling-moment data at the start and
at the end of the vibration period are presented in figures 10(a)
and 10(b), respectively. It is believed that the amplitude of the
wing vibration as shown by these data represents approximately
50 percent of the actual magnitude. The exact percentage is not
definitely known however because a frequency response test of the
recording instrument was not made at the time of the flight but
at some time afterwards, and the instrument characteristics may
be subject to change over a period of time. The modulation of the
rolling-moment record, prevalent except for the last half second
of the vibration period, is believed to be due to deficiencies in
the recording equipment when operating at frequencies outside of
its design range.

The frequency characteristics of the wing and aileron vibration
are shown plotted against Mach number in figure 11. These data
show the wing and ailerons vibrated at the same frequency for any
given Mach number and that the frequency of the wing and aileron
oscillations increased with increase of Mach number.

The flutter speed of swept-back wings of the type used on
the RM-1 cannot be calculated at present. Vibration tests were
therefore made on a wing rolling-moment balance setup identical
to that used on the model reported herein. These tests showed
that the first symmetrical bending frequency was 21 cycles
per second with the node at the root chord and that the symmetrical
torsion frequency was 75 cycles per second with the node line
approximately parallel to the leading edge and at a distance of
48 percent of the wing chord behind it. In the simplest type of
classical wing flutter, the flutter frequency would be expected to
lie between those of first bending and first torsion frequencies.
However, the frequencies of the vibrations recorded in the flight
tests (90 to 120 cycles per second) were considerably higher than

the wing structure frequencies measured. It is probable therefore that the flight oscillations did not represent a classical flutter condition but rather were associated with the phenomenon known as "aileron buzz" or aileron compressibility flutter hitherto encountered only on straight wing-aileron combinations of nonsymmetrical airfoil section, at supercritical speeds. Flight tests of a Bell P-63A-6 airplane reported in reference 4 and wind-tunnel tests of a modern high-speed-airplane wing made in the Ames 16-foot high-speed tunnel show aileron and wing oscillations at high speed similar to those observed in the subject test. It is believed that aileron compressibility flutter is associated with a coupling of the variations of the relative intensities of the upper-surface and lower-surface shock waves with aileron motion. The condition might be considered to be a flutter condition requiring only one degree of freedom, that is, aileron rotation about its hinge line. The wing oscillation is believed to the the result of flow and load changes induced by the aileron and in the case of the FM-1 model was probably amplified in intensity by the flexibility of the wing and rolling-moment balance system.

It is deduced from the RM-1 test data that aileron compressibility flutter is not dependent upon camber for its appearance and that its appearance is delayed, but not prevented by use of sweepback.

The data in figure 10(b) show that both the wing and aileron oscillations stop at approximately the same Mach number (1.03) at which the ailerons regained control on the RM-1 flight reported in reference 1. As the velocity was reduced past the velocity corresponding to this value, the aileron did not show the large degree of overbalance noted at near-critical speeds in accelerated flight but instead appeared to regain its subsonic characteristics without appreciable transition. It is possible that the violent aileron oscillation in the supersonic region may have damaged the control-position indicator causing faulty readings. Another more likely explanation may be that shock conditions on the wing do not disappear in the same manner in which they are formed. It may be that the wing shock waves vanish abruptly as the velocity is decreased through the critical speed rather than by a gradual process of weakening intensity. Such procedure would explain the aileron behavior of the RM-1 model at transonic and subsonic velocities in coasting flight.

CONCLUSIONS

Based on free-floating aileron data obtained in a flight test
of a supersonic research pilotless aircraft, the following
conclusions are drawn:

1. A large-amplitude high-frequency oscillation of the aileron
and wing was encountered in the supersonic region on a swept-back
wing with a free-floating aileron having a high degree of aero-
dynamic balance and complete mass balance.

2. The frequency of the oscillations increased with increase
of velocity, rising from a value of 90 cycles per second near a
Mach number of 1.0 to 120 cycles per second at a Mach number of 1.4.

3. The flutter observed in the subject test is similar in
nature to the phenomenon called aileron compressibility flutter
hitherto observed on high-speed straight-wing aircraft of
nonsymmetrical section flying at or above their critical velocity.
It is thus indicated that aileron compressibility flutter is not
dependent upon camber for its occurrence and is primarily a
Mach number effect which may be delayed, but not prevented, by
use of sweepback.

4. At high subsonic velocities the bevel-edged aileron, although
underbalanced at large deflections, was overbalanced at small
deflections.

5. The data indicate that the aileron became strongly over-
balanced as the critical velocity was approached. This effect
was reversed when supercritical velocities were attained, the
aileron becoming very stiff (underbalanced) in the supersonic region.

Langley Memorial Aeronautical Laboratory
    National Advisory Committee for Aeronautics
        Langley Field, Va.

REFERENCES

1. Pitkin, Marvin, Gardner, William N., and Curfman, Howard J., Jr.:
     Results of Preliminary Flight Investigation of Aerodynamic
     Characteristics of the NACA Two-Stage Supersonic Research
     Model RM-1 Stabilized in Roll at Transonic and Supersonic
     Velocities. NACA RM No. L6J23, 1946.

2. Mendelsohn, Robert A.: Wind-Tunnel Investigation of the
     Boundary Layer and Wake and Their Relation to Airfoil
     Characteristics - NACA 65_1-012 Airfoil with a True-Contour
     Flap and a Beveled-Trailing-Edge Flap. NACA MR No. L6G15, 1946.

3. Langley Research Department: Summary of Lateral Control
     Research. (Compiled by Thomas A. Toll.) NACA TN No. 1245, 1947.

4. Spreiter, John R., and Galster, George M.: Observations of
     Aileron Flutter on the Bell P-63A-6 Airplane in Flight
     at High Mach Numbers. NACA ACR No. 6B08, 1946.
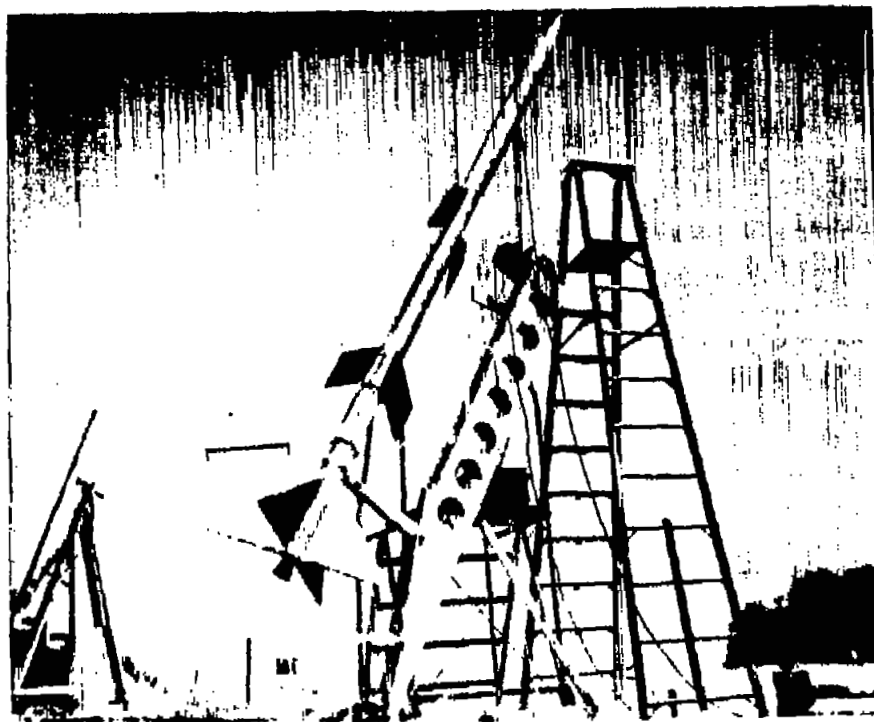
Figure 1.- RM-1 with booster mounted on launching rack.

Fig. 1

Figure 2.- RM-1 wing-aileron combination.

Fig. 2

NACA 65-010

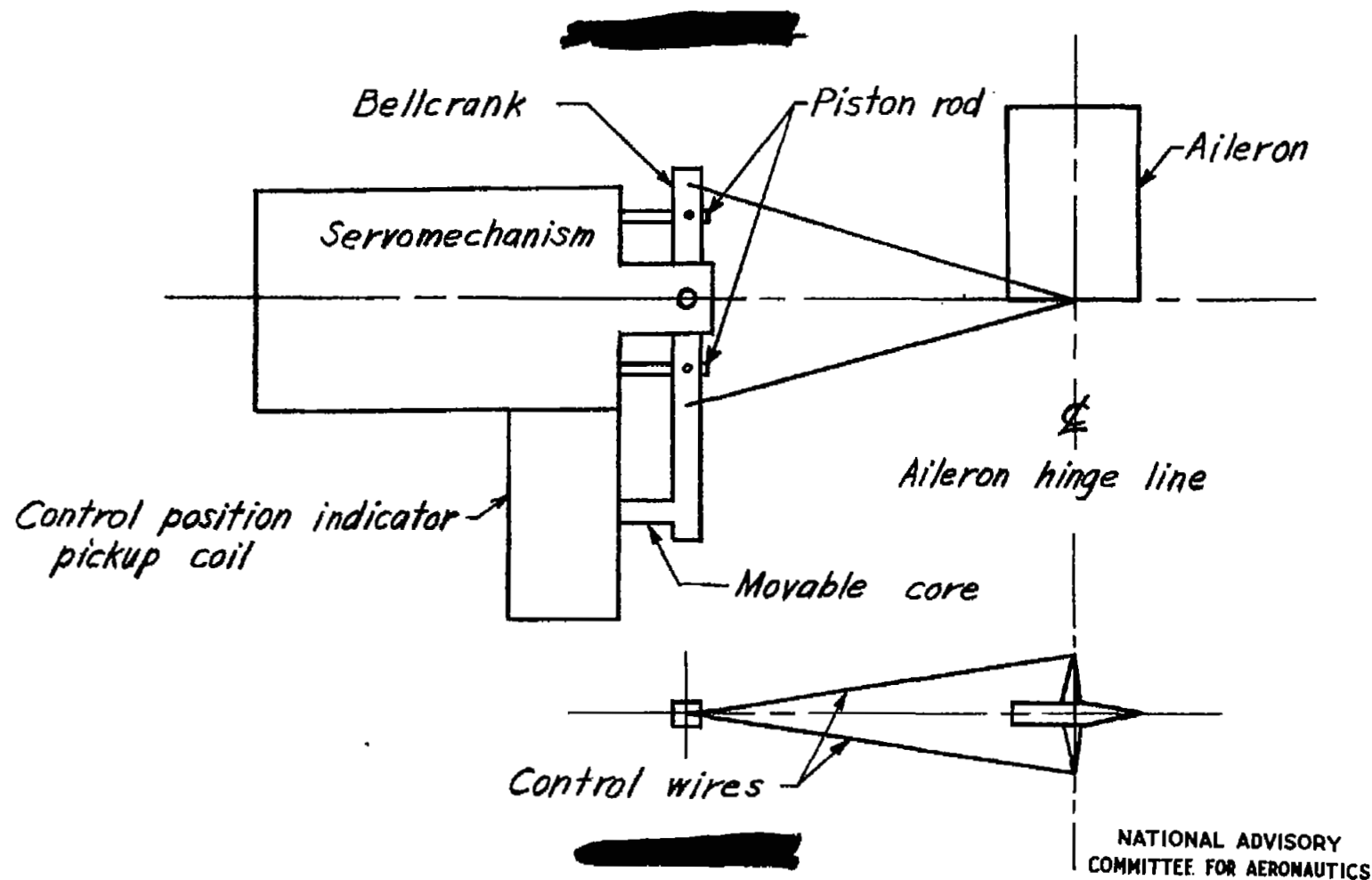Center line of model

A-A

NATIONAL ADVISORY
COMMITTEE FOR AERONAUTICS
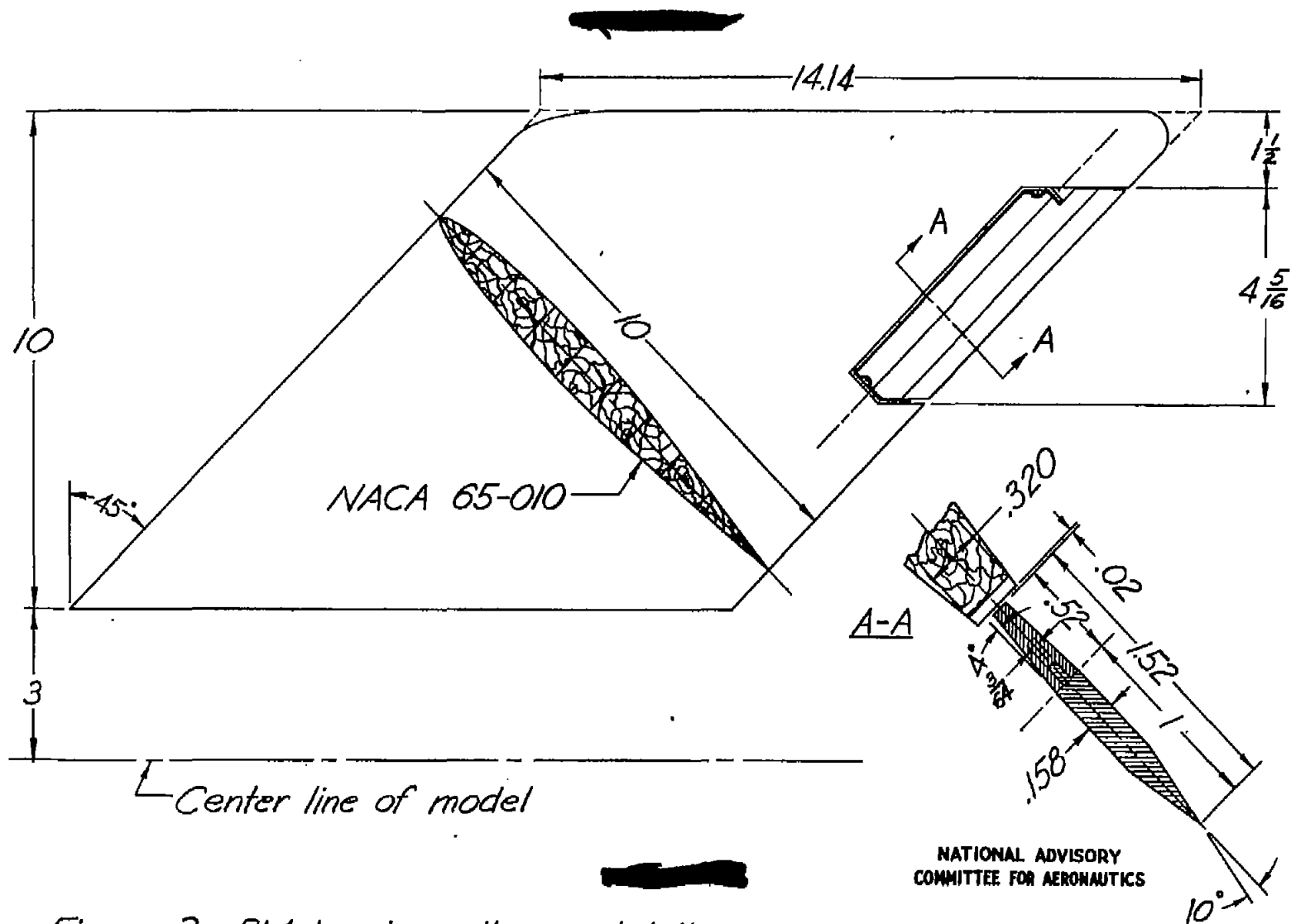
Figure 3.- RM-1 wing-aileron detail.

Fig. 3

Fig. 4

Bellcrank

Piston rod

Aileron

Servomechanism

Control position indicator
pickup coil

Aileron hinge line

Movable core

Control wires

NATIONAL ADVISORY
COMMITTEE FOR AERONAUTICS

Figure 4.— Schematic sketch of aileron, servomechanism, and control
position indicator arrangement.

- Wings with ailerons
- Balance beam
- Extension arm
- Telemeter pick-up coil
- Movable core
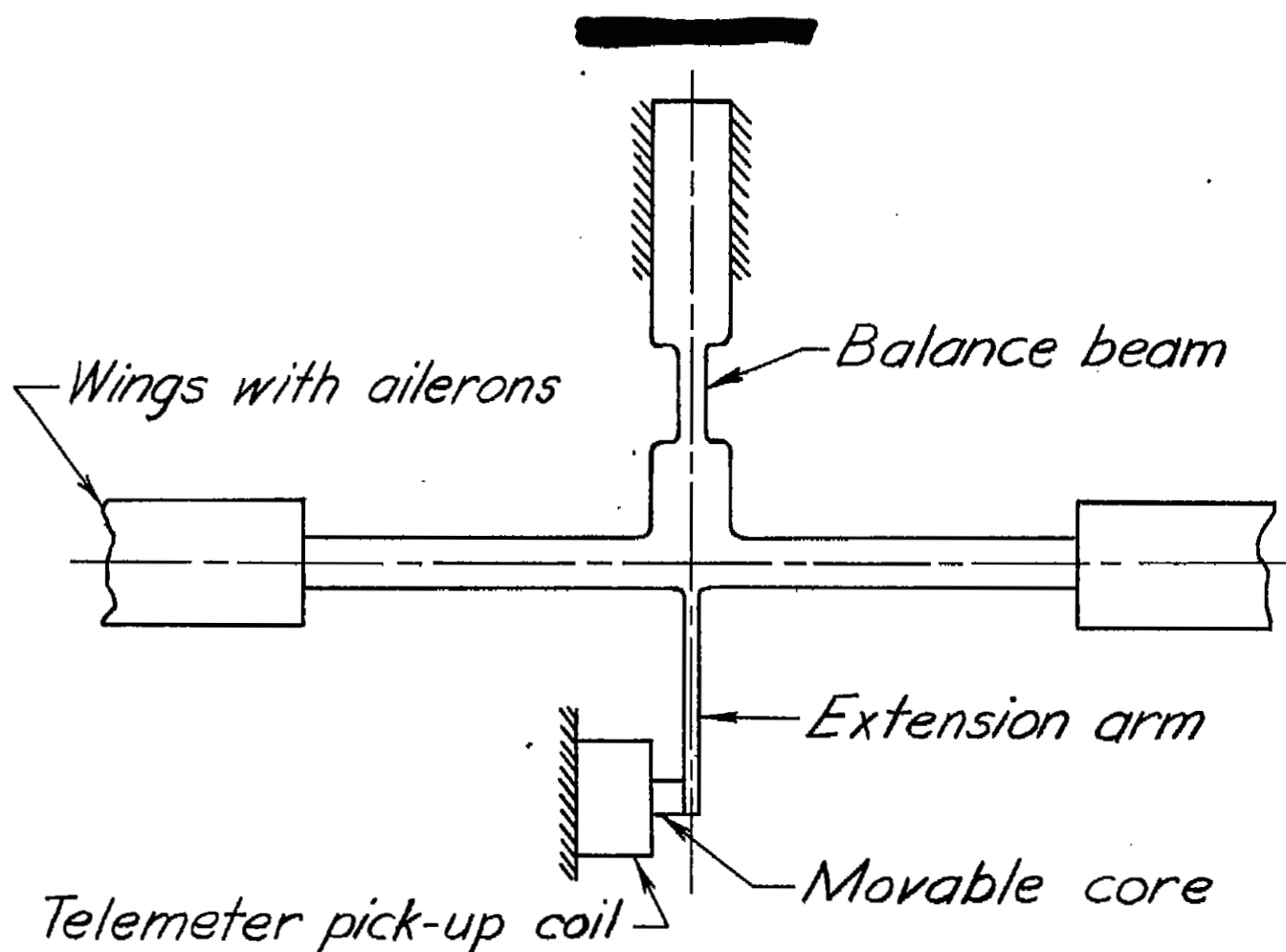
Figure 5.- Sketch of rolling-moment balance system.

Fig. 5

Fig. 6
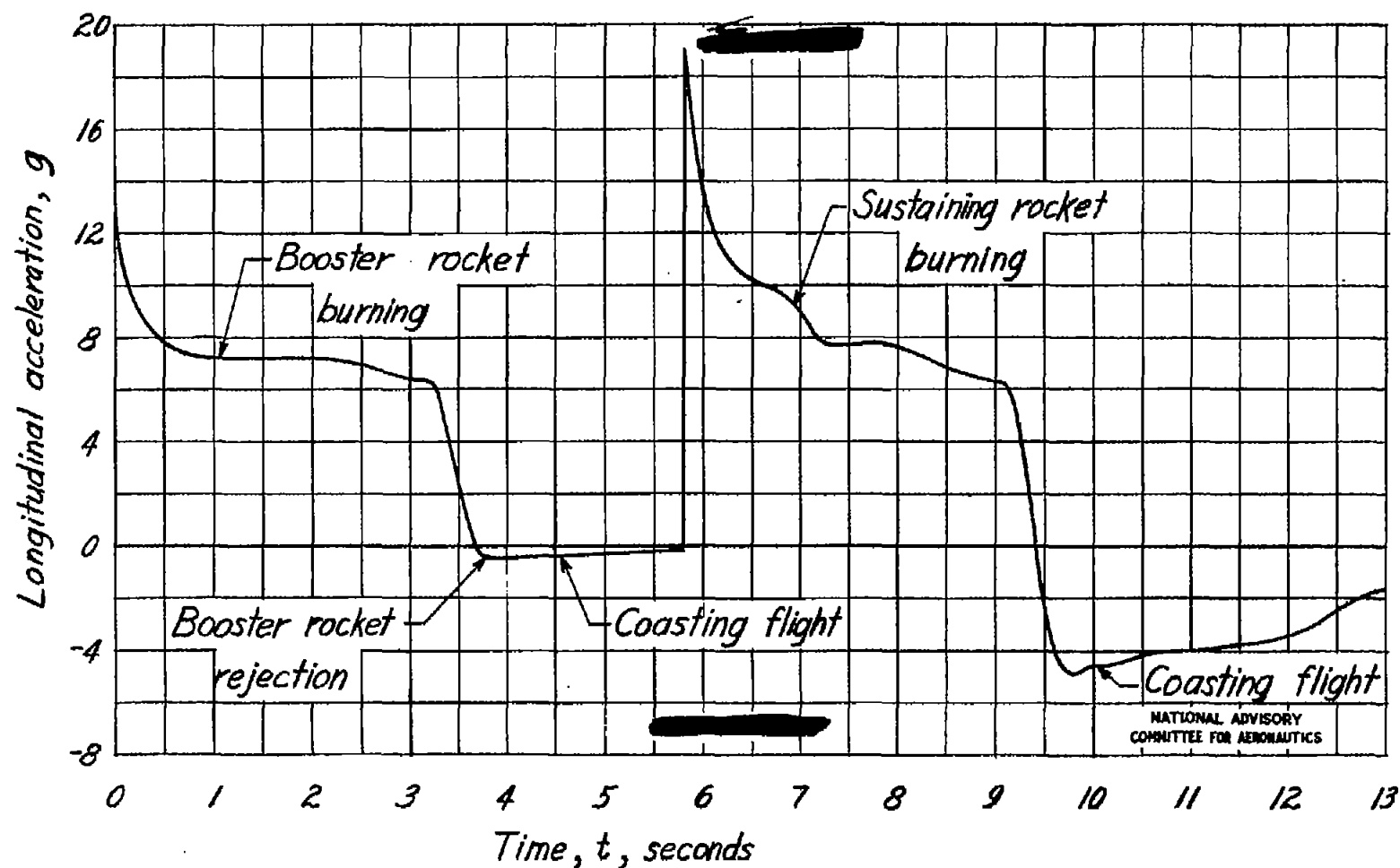
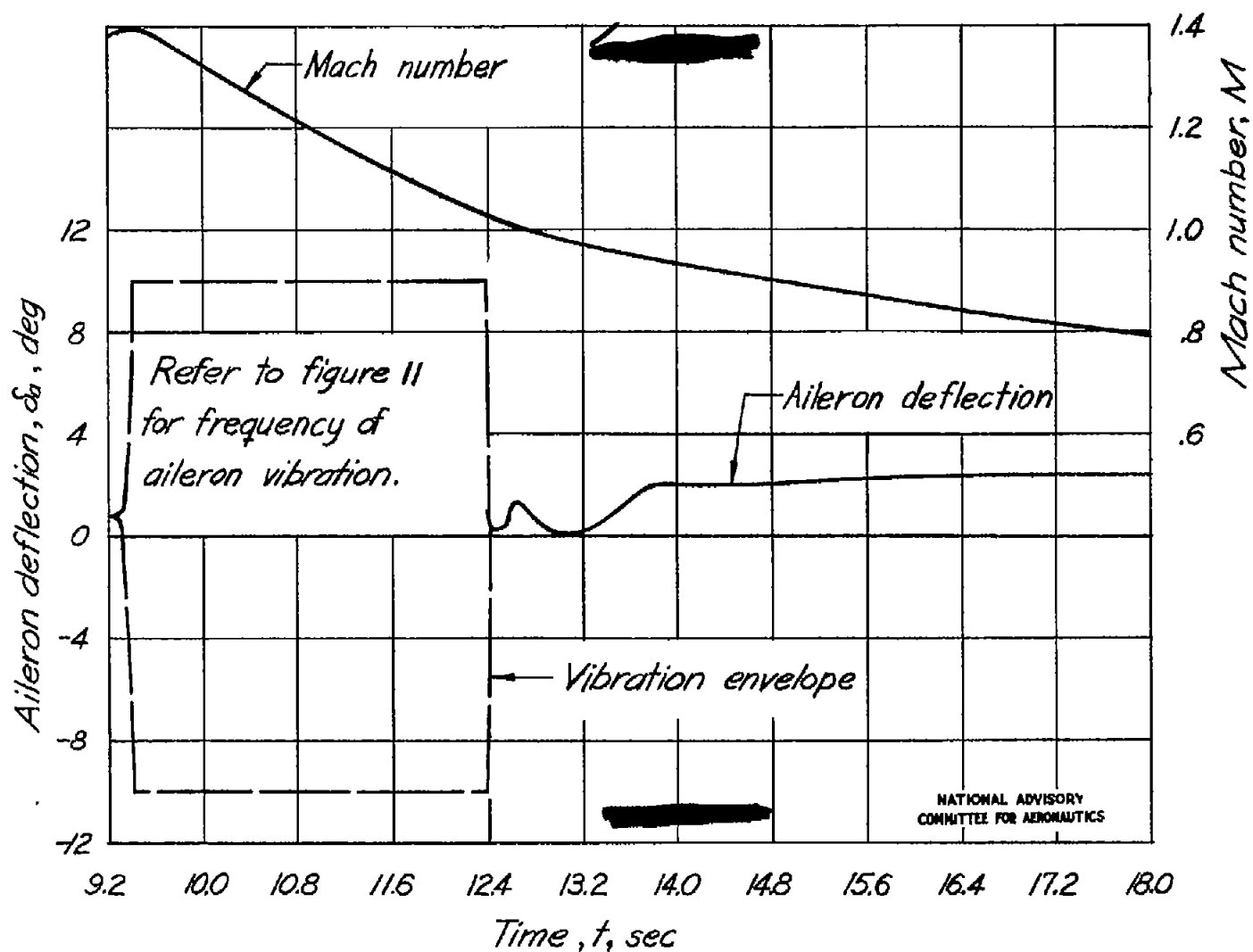Figure 6. — Longitudinal acceleration variation with time.
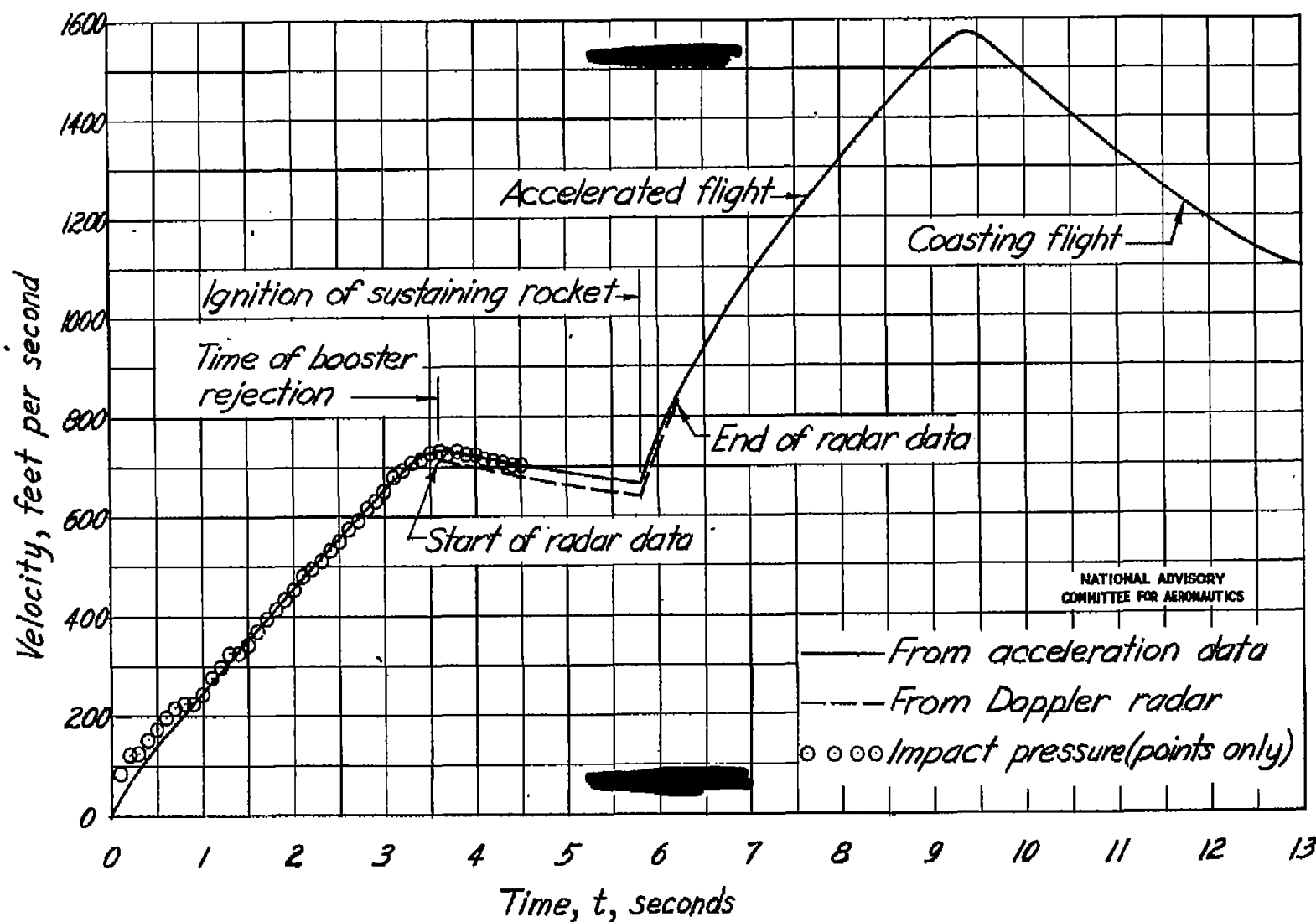
Figure 7.-Velocity variation with time.

Fig. 7
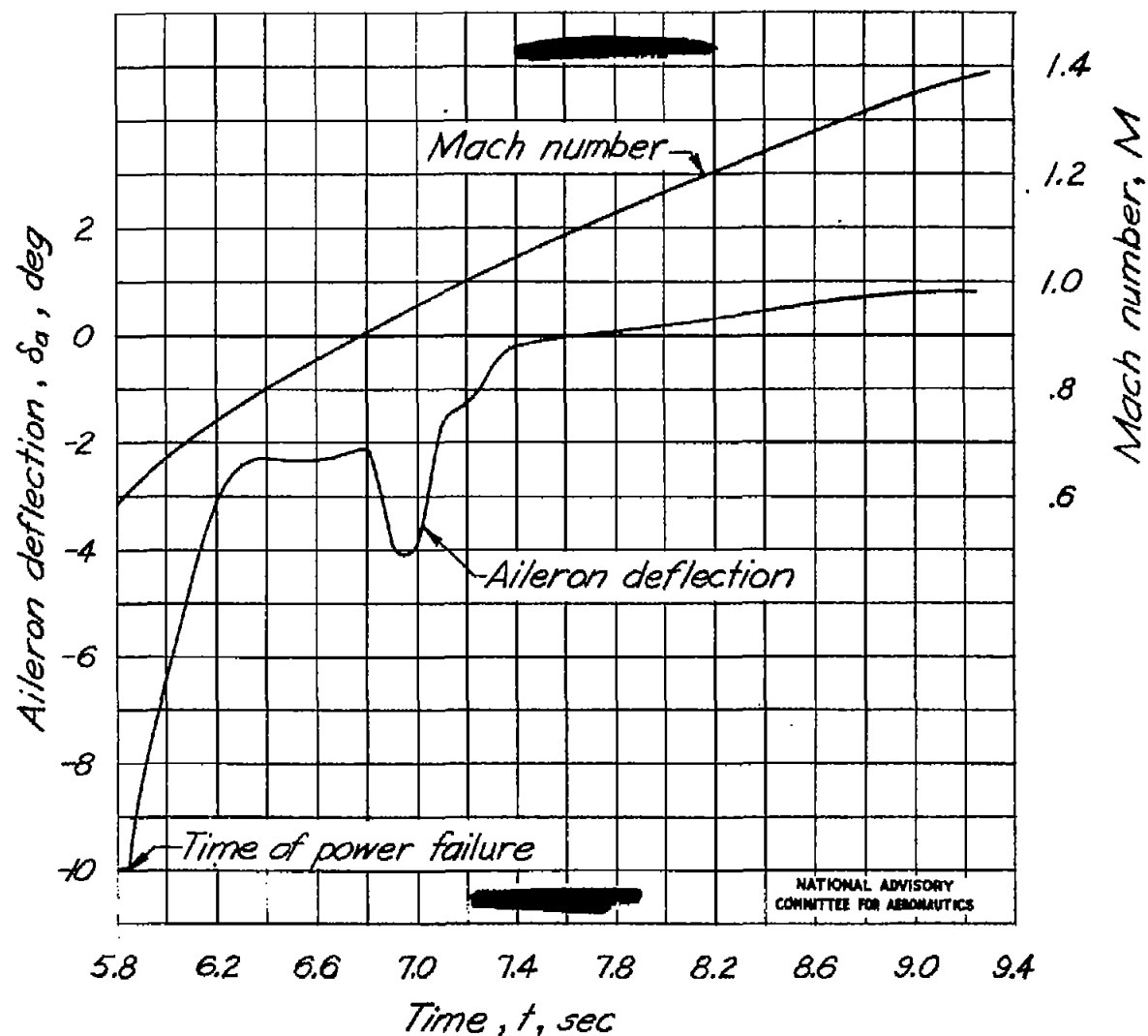
(a) Aileron deflection and Mach number against time.

Figure 8 .– Aileron characteristics in accelerated flight.
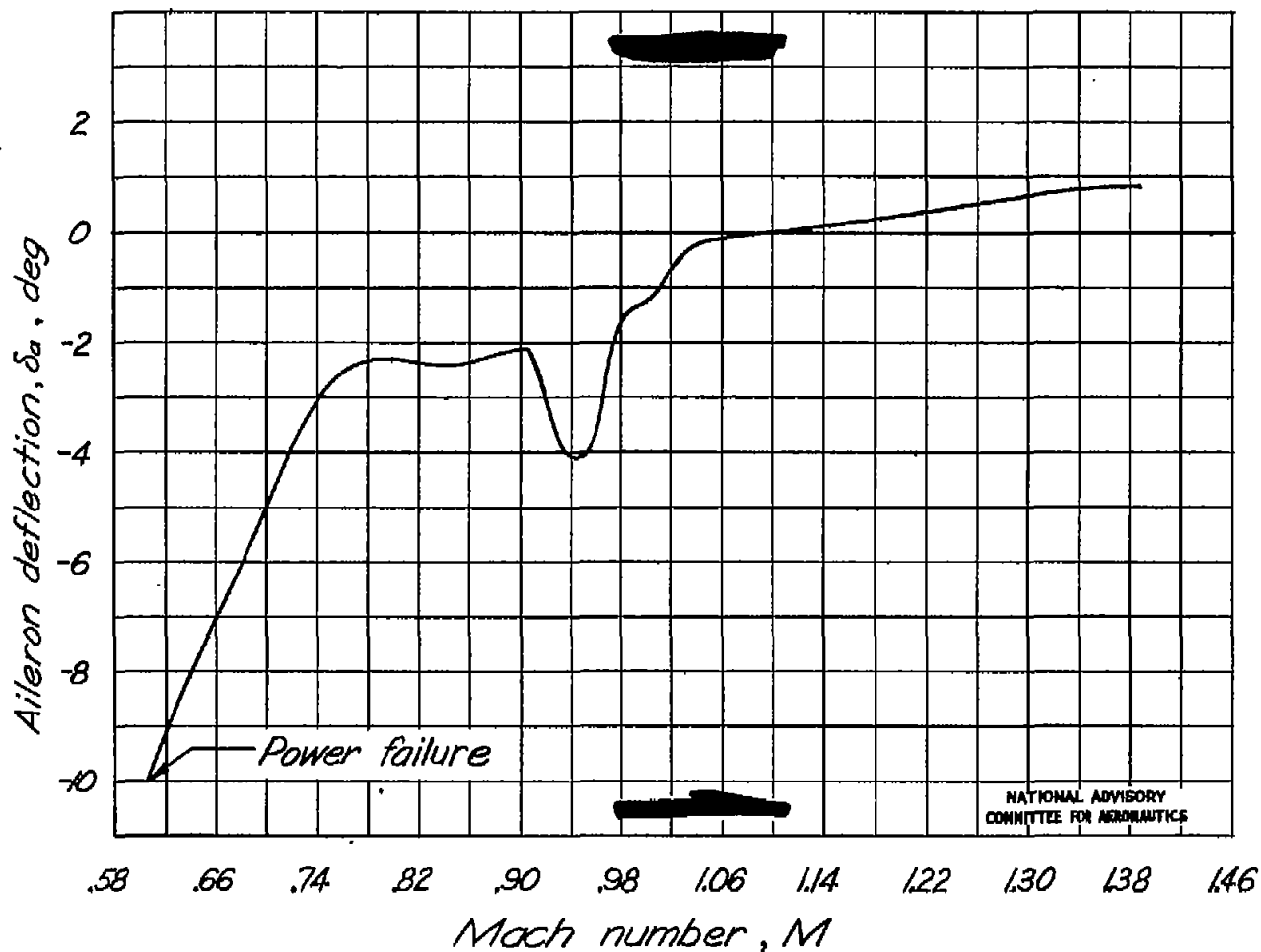
(b) Aileron deflection – Mach number.

Figure 8. – Concluded.

Mach number

Refer to figure 11 for frequency of aileron vibration.

Aileron deflection

Vibration envelope

NATIONAL ADVISORY
COMMITTEE FOR AERONAUTICS

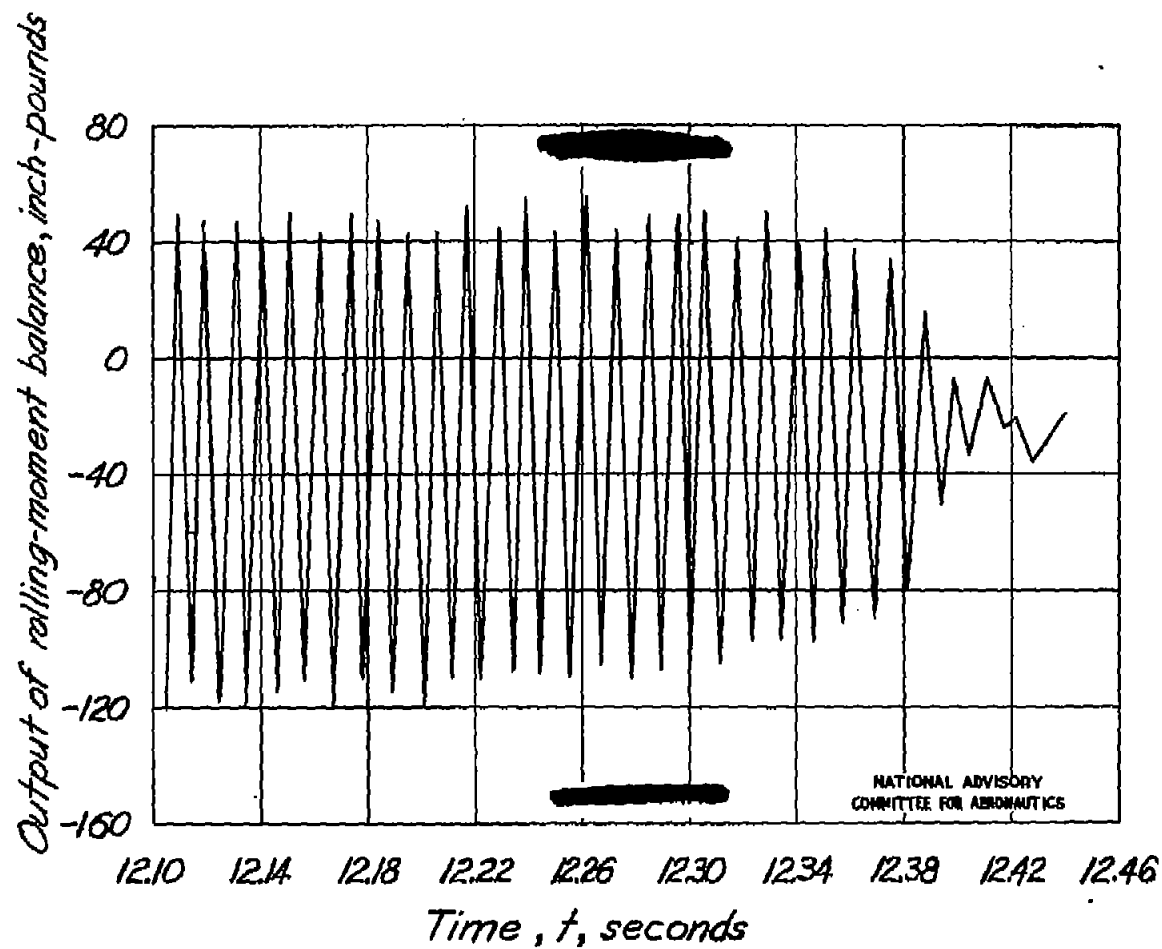Aileron deflection, δ_a, deg

Mach number, M

Time, t, sec

(a) Aileron deflection and Mach number against time.

Figure 9. - Aileron characteristics in coasting flight.
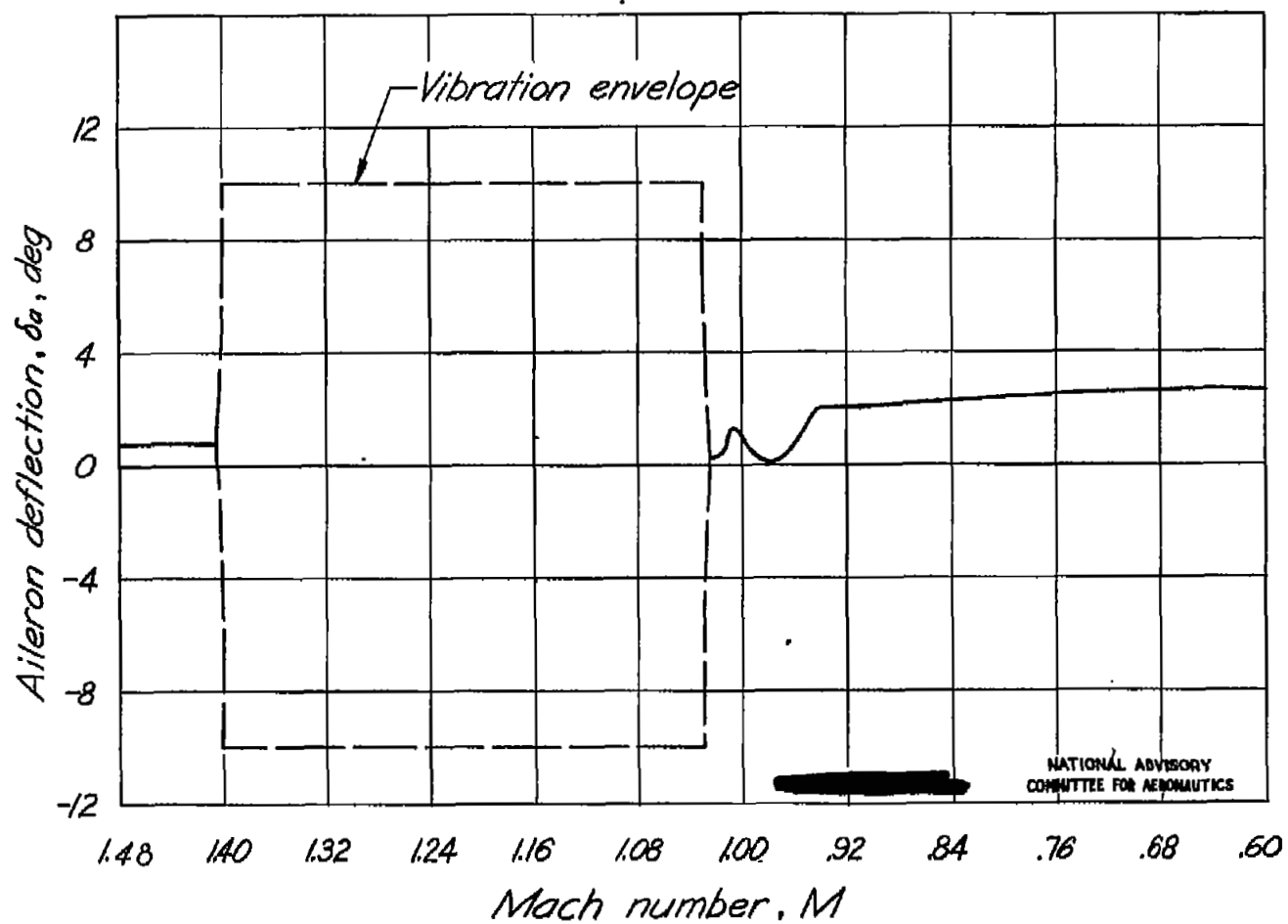
(b) Aileron deflection – Mach number.

Figure 9. – Concluded.

NATIONAL ADVISORY
COMMITTEE FOR AERONAUTICS
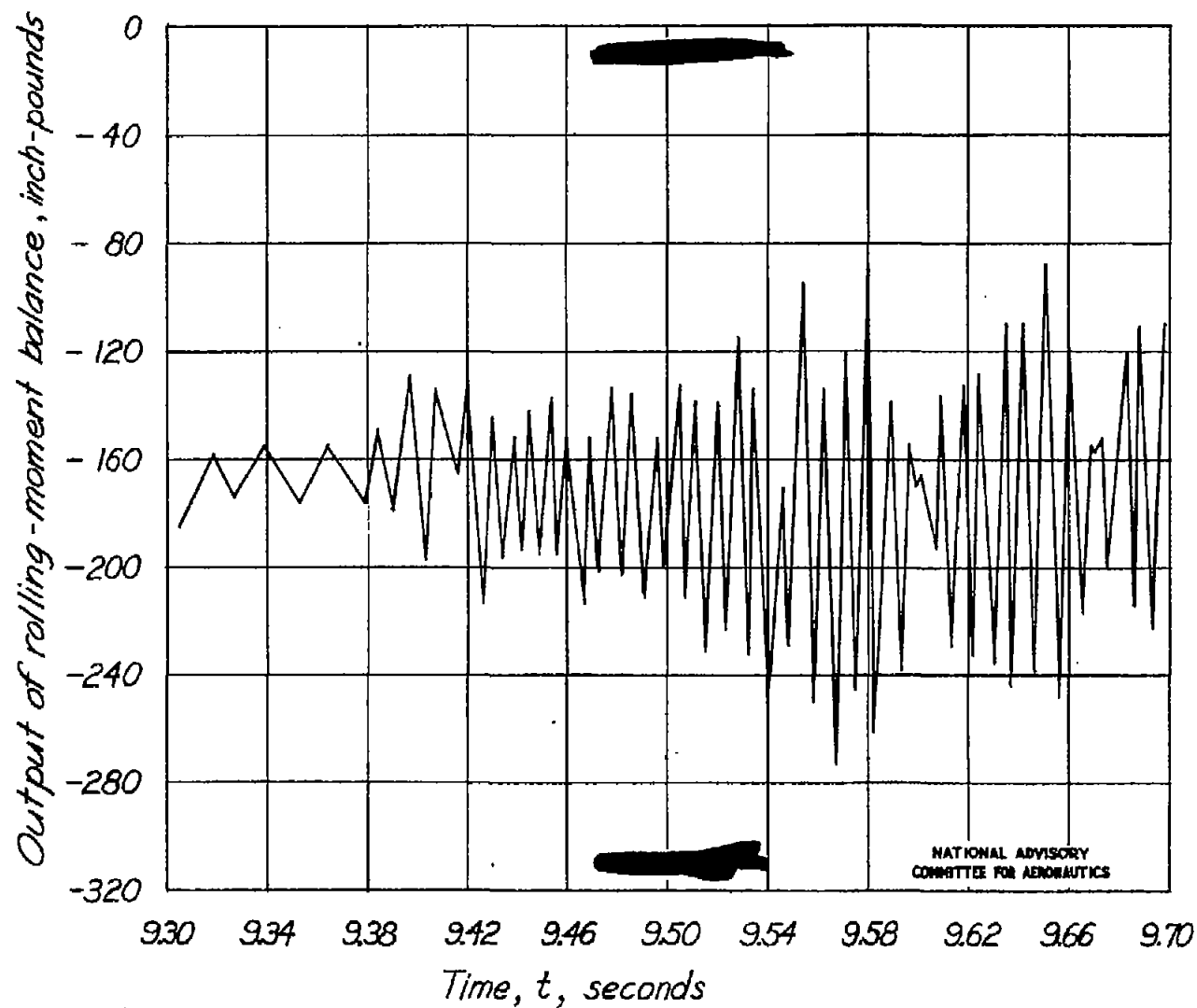
(a) Start of vibration period.

Figure 10. – Time history of rolling-moment balance vibration.

(b) End of vibration period.

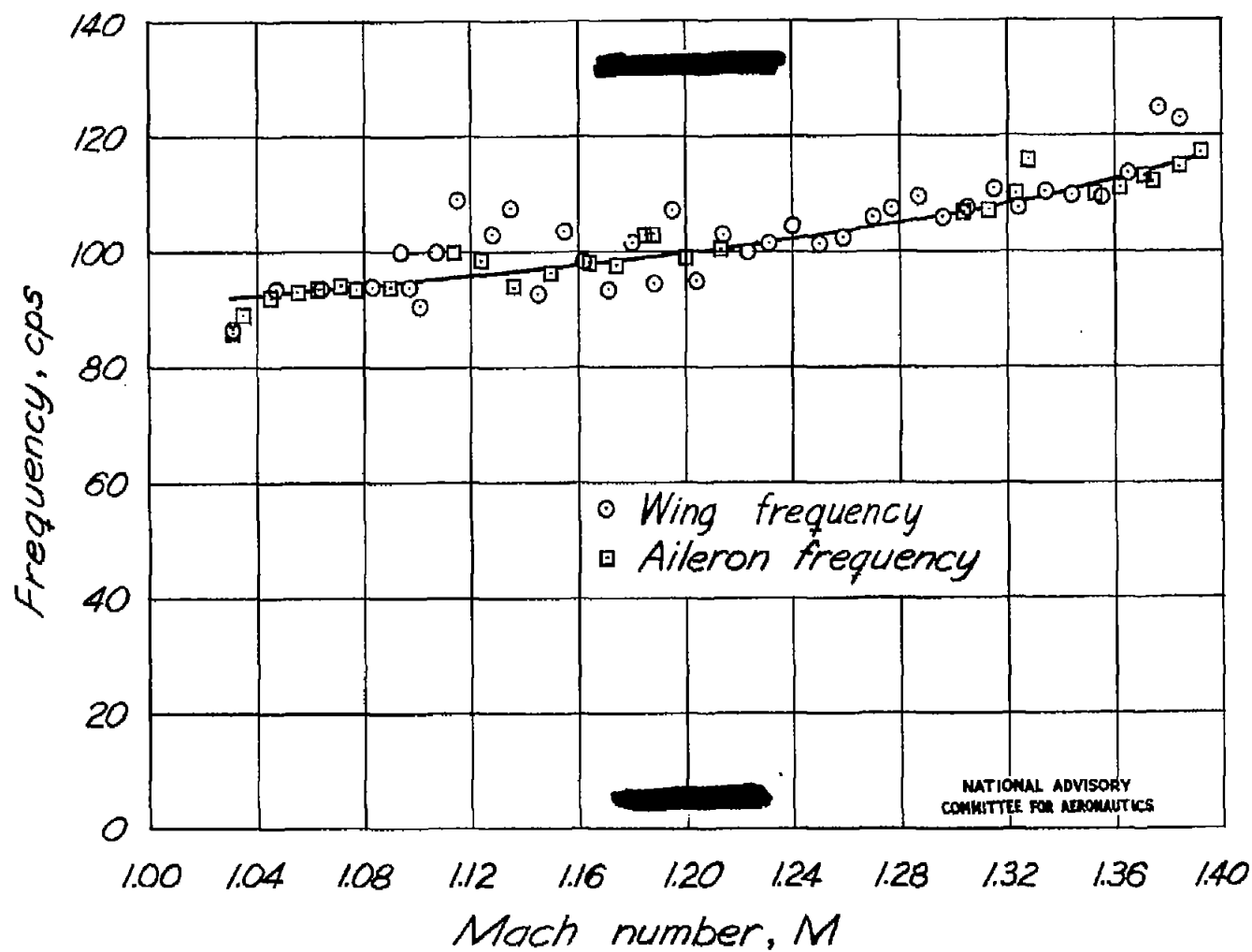Figure 10. – Concluded.

Fig. 11

Figure 11.-Variation of wing and aileron vibration frequencies with Mach number.